ASSESSMENT OF GROUND SURFACE DEFORMATION IN BENGKULU CITY INDUCED BY EARTHQUAKES USING DINSAR-BASED REMOTE SENSING IMAGE ANALYSIS

Ferzha Putra Utama[1,*], Arie Vatresia[2], Lindung Zalbuin Mase[3], Ahmad Faris[2]

[1]Department of Information System, Faculty of Engineering, University of Bengkulu
[2]Department of Informatics, Faculty of Engineering, University of Bengkulu
[3]Department of Civil Engineering, Faculty of Engineering, University of Bengkulu

*e-mail: fputama@unib.ac.id

Abstract. In 2007, Bengkulu city, Indonesia and its surrounding areas experienced a significant earthquake with a magnitude of 8.6 M_w, resulting in extensive damage. Between 2014 and 2022, Bengkulu Province encountered a total of 3469 earthquakes, signifying a heightened frequency of seismic activity in the region. This escalated seismic activity in Bengkulu elicits concerns regarding potential ground surface deformation. To address this, the study utilized DInSAR (Differential Interferometry SAR) technology, employing a blend of satellite images to quantify land surface deformation. Notably, the research made use of three pairs of satellite images for analysis. One pair of ALOS-PALSAR images dated between January 29 and September 16, 2007, was employed to investigate ground surface deformation following the September 12, 2007 earthquake. Additionally, observations were made using two pairs of Sentinel-1 satellite images covering periods from November 3 to 27, 2014, and from June 30 to July 24, 2022, to monitor land surface deformation resulting from earthquakes on November 10, 2014 and July 20, 2022. The study findings depicted uplift deformation reaching 53.4 mm and the highest subsidence measuring -12.8 mm in the ALOS-PALSAR image pair. In the Sentinel-1 image pair between November 3 and 27, 2014, the most notable observed uplift amounted to 38.9 mm, while the greatest subsidence was recorded at -34.8 mm. Lastly, the image pair dated between June 30 and July 24, 2022, exclusively exhibited uplift, with values peaking at 45.2 mm.

Keywords: *Bengkulu, deformation, DInSAR, earthquake, Sentinel-1*

1 INTRODUCTION

Bengkulu is a city in Indonesia located in an area with significant geological activity due to its proximity to the subduction zone plate between the Indo-Australian and Eurasian plates, as well as the Musi and Manna segment faults. These conditions result in frequent plate shifts and earthquakes. Since 2000, there have been at least two earthquakes with a magnitude higher than 7 Mw, emphasizing the importance of preparedness and infrastructure to mitigate the impact of future seismic events. Specifically, a 7.9 M_w earthquake occurred on June 4, 2000, followed by an 8.6 M_w earthquake on September 12, 2007 (Mase, 2018, 2020; Mase et al., 2024). The major earthquake triggered widespread panic among the public, leading to chaotic scenes as people rushed to find safety. Many buildings suffered significant damage, with some collapsing entirely. Landslides occurred in hilly areas, posing additional dangers to residents. The earthquake also severely affected public infrastructure, disrupting transportation and utilities. In some locations, the ground turned unstable due to liquefaction, compounding the destruction and creating hazardous conditions (Mase, 2023, 2024).

According to data released by the Meteorology, Climatology, and Geophysics Agency (BMKG) in 2022, Bengkulu province experienced a total of 2,989 earthquakes with a magnitude of 3 or above between 2000 and 2021 (Vatresia et al., 2024). Subsequent data from BMKG Bengkulu Province revealed that 3,469 earthquakes occurred within the province from 2014 to 2022. Notably, 238 earthquakes were recorded in 2014, with one significant event taking place on November 10, 2014, registering a magnitude of 4.8. This earthquake was strongly felt by the local community due to its epicenter's proximity, located just 66 km southwest of Bengkulu Utara, and with a shallow depth of only 20 km beneath the surface.

The occurrence of destructive earthquakes does not fully raise awareness among the government, property developers, and the community regarding the importance of selecting appropriate locations for building construction. Weak regulations and low land prices in areas with unstable soil are leading to haphazard and uncontrolled housing development. Despite the evident risks posed by unstable soils and seismic activity, economic factors often overshadow safety considerations. The absence of stringent land-use policies and enforcement mechanisms exacerbates this issue, enabling the proliferation of structures in high-risk zones. Additionally, there is limited public knowledge about geological hazards, which hinders informed decision-making regarding safe building practices. To address these challenges, governments must implement and enforce stricter building codes and land-use regulations, coupled with public awareness campaigns on the importance of seismic safety. Moreover, integrating geospatial technologies, such as DInSAR, into urban planning can help identify and map vulnerable areas, guiding safer and more sustainable development practices.

The analysis of ground surface deformation in Bengkulu is crucial for identifying seismic micro-zones to facilitate the development of seismic hazard maps. Implementation of geotechnical measurements in the field for this analysis demands substantial resources, encompassing financial investment, advanced technology, and skilled personnel (Sattler et al., 2022; Yang et al., 2022). This study aims to offer a more straightforward approach for observing changes in land surface conditions that may have occurred subsequent to an earthquake. An alternative approach involves harnessing satellite image data and information technology to conduct preliminary analysis, preceding field verification with geotechnical methods. Radar-based remote sensing satellite technology, such as SAR (Synthetic Aperture Radar), can be utilized to observe land surface deformation by examining changes in the position of objects in relation to the Line of Sight (LOS), and identify uplift or subsidence of the land surface (Li et al., 2021; Razi et al., 2023; Usman et al., 2022). Researchers have successfully

employed GPS, InSAR, and DInSAR (Differential Interferometry Synthetic Aperture Radar) technologies to study land surface deformation in diverse regions (Fielding et al., 2020; Kandregula et al., 2022; Lakhote et al., 2021).

Measuring ground surface deformation in Bengkulu is crucial due to its vulnerability to earthquakes. These measurements are vital for assessing earthquake susceptibility and formulating disaster mitigation plans. Utilizing the DInSAR method allows for comprehensive temporal observation and analysis of ground surface deformation. Therefore, it is imperative to conduct an analysis of land surface deformation in Bengkulu using DInSAR-based remote sensing image processing (Differential Interferometry Synthetic Aperture Radar) to identify changes in land surface conditions, delineate earthquake-prone areas, and facilitate the development of earthquake disaster mitigation strategies.

Although the DInSAR method has some shortcomings, including atmospheric interference, loss of coherence in vegetated areas, and challenges in capturing rapid deformation due to low temporal resolution, it remains a promising technique. The availability of abundant and freely accessible satellite radar data, such as that from Sentinel-1, adds significant value to its use. Additionally, DInSAR can serve as a thorough initial study to identify changes in land surface conditions and to detect earthquake-prone areas.

2 MATERIALS AND METHODOLOGY

2.1 Study Area

Bengkulu, located on the island of Sumatra, is situated near the subduction zone of the Eurasian and Indo-Australian plates. Bengkulu City is geographically located between 3045-3059 S and 102°14′–102°22′ E. As depicted in Figure 2-1, Bengkulu is also close to several major Sumatran faults, including the Manna segment and Musi segment faults. As a result, it is important to take proactive measures to mitigate the vulnerability of Bengkulu to earthquakes given its susceptible location. This area has experienced significant seismic activity in the past, highlighting the importance of preparedness and resilience (Murjaya et al., 2023).

While there are few studies directly addressing earthquakes and their effects on the ground level in Bengkulu, several research efforts have utilized remote sensing to monitor areas near Bengkulu following natural disasters (Hakim & Lee, 2020). Previous investigations have also examined land changes in Bengkulu caused by earthquakes and tsunami waves (Anggara et al., 2025; Gusman et al., 2010). These findings offer valuable insights for expanding research on earthquake incidents in Bengkulu over a more extended time period.

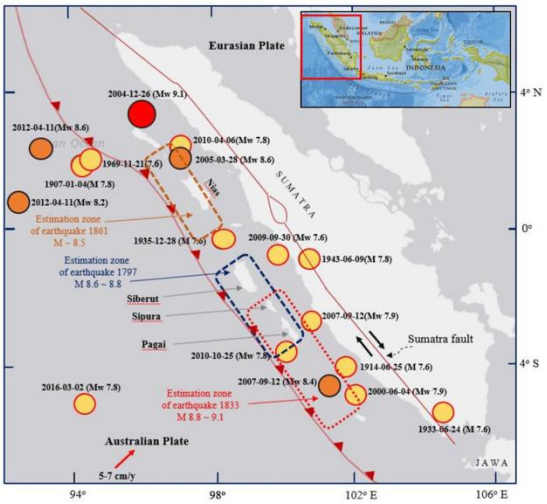

Figure 2-1: Seismic activity, and estimated rupture areas of major intraplate earthquakes along the Sunda megathrust from 1900 to 2019. The circles represent different earthquake magnitudes: red for $M_w \geq 9.0$, brown for $8.0 \leq M_w < 9.0$, and yellow for $7.5 \leq M_w < 8.0$.

2.2 Data

The data incorporated in this study consist of ALOS PALSAR satellite imagery, Sentinel-1 data, Precise Orbit Ephemerides (AUX_PEORB) data, Shuttle Radar Topography Mission (SRTM) Digital Elevation Models (DEMs), and earthquake event data from Bengkulu City covering the years 2007 to 2023. The ALOS PALSAR satellite images analyzed in this research include a Level 0 image captured on January 29, 2007 (Scene ID: ALPSRP054057100), and another image taken on September 16,

2007 (Scene ID: ALPSRP087607100). ALOS PALSAR images, with a detailed resolution of 50 m corresponding to each pixel representing 250 m^2, were used to meticulously examine the ground surface deformation caused by the powerful 8.6 magnitude earthquake that rocked the area on September 12, 2007.

Furthermore, the study incorporated the intricate analysis of two pairs of Sentinel-1 level 1.0 (Single Look Complex) images. The first pair, captured between November 3, 2014, and November 27, 2014, provided a close look at the deformation patterns triggered by the 4.7 magnitude earthquake on November 10, 2014. The second pair, between June 30 and July 24, 2022, was scrutinized to observe the ground surface deformation following the 5.8 magnitude earthquake that occurred on July 20, 2022. Sentinel-1 images, distinguished by their high resolution of 10 m, made it possible to analyze changes at a granular level, with each pixel representing 100 m^2.

This study utilizes two types of SRTM data: the 30-meter resolution DEM and the 90-meter resolution DEM, both of which encompass the entire area of Bengkulu City. The 90-meter SRTM DEM was employed to reduce topographic effects on the ALOS PALSAR imagery, while the 30-meter SRTM DEM was utilized to correct for topographic influences on the Sentinel-1 imagery.

2.3 Methods

To facilitate data processing, radar satellite image data from ALOS-PALSAR and Sentinel-1A, both in Single Look Complex (SLC) format, are used. The initial phase involves preparing two satellite images (referred to as the master image and the slave image) that capture the same geographic area at different time intervals. Using the InSAR method, these images are processed to produce interferograms. The next step includes a differencing process, resulting in a differenced interferogram.

Since the resultant interferogram may still contain topographic effects, Differential InSAR (DInSAR) processing requires the integration of Digital Elevation Model (DEM) data from the Shuttle Radar Topographic Mission (SRTM) to mitigate these effects. Additionally, DInSAR analysis has limitations, such as atmospheric disturbances and vegetation-induced coherence loss, which can reduce the accuracy of deformation measurements. To address these challenges, atmospheric corrections can be applied using external models, such as weather data or persistent scatterer methods. For vegetation-related coherence loss, optimizing temporal and spatial baselines is crucial, in conjunction with advanced coherence estimation techniques. Importantly, the DInSAR process culminates in an interferogram with a coherence value ranging from 0 to 1, indicating the quality of the measurement, as illustrated in Figure 2-2 (Bayik, 2021; Goorabi, 2020; Nurtyawan & Yulanda, 2020; Suhadha & Julzarika, 2022). Notably, a coherence value of 1 indicates the congruence of the master and slave images used. A favorable coherence value typically ranges from at least 0.2 to a proximity of 1.

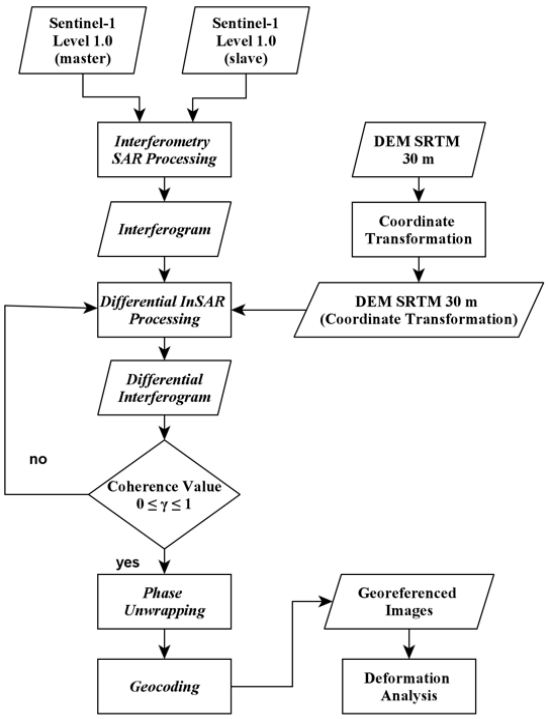

Figure 2-2: Research Flowchart

The problem of ambiguity arises due to the interferogram produced from the DInSAR process still being in radian units (phase angle units) within the range of -π to π. Although the

deformation pattern is visible, the information about the deformation value cannot be properly interpreted. The unwrapping process is conducted to convert the absolute phase angle unit into a metric unit within the interferogram, resulting in a deformation image with values that are easier to interpret. In the subsequent phase, the geocoding process entails the conversion of the radar coordinate system within the interferogram into a geographic coordinate system. This transformation is essential to ensure that every pixel in the resultant interferogram accurately corresponds to a specific location on the earth's surface. The unwrapping and geocoding processes were effectively executed using GMTSAR on a Linux platform, which allowed for precise data handling. Following these crucial steps, we focused on crafting a comprehensive map layout using ArcGIS. Figure 2-2 is the flowchart illustrates that the outcome of the geocoding process yields an image already integrated with a geographic coordinate system. The final stage encompasses the deformation analysis, with the objective of ascertaining the magnitude of the deformation and comparing these values across the various earthquake events under study. The findings of this study will be validated by geotechnics researchers to minimize the margin of error.

3 RESULTS AND DISCUSSION

Deformation on the Earth's surface can occur significantly or gradually over time. To assess land surface deformation caused by earthquakes, it is essential to have images captured shortly before and after the seismic event. The coherence value in forming interferogram images is influenced by the perpendicular baseline and temporal baseline. In order to achieve a high coherence value on Sentinel-1 images, it is necessary to maintain a baseline length of no more than 150 meters and a temporal distance of no more than 6 months. However, for ALOS PALSAR images, there is currently no specific data regarding the optimal baseline value required to produce a high-quality interferogram.

3.1 InSAR and DInSAR Processed Images

The image data utilized in SAR processing using GMTSAR (Asset et al., 2021) provides the temporal baseline and perpendicular baseline, which are detailed in Table 3-1 for reference. In Table 3-1, the perpendicular baseline lengths for the image pairs from the 2007, 2014, and 2022 earthquake events, formed into an interferogram, were as follows: -670.83 m (image pair January 2007 - October 2007), -64.74 m (image pair November 3, 2014 - November 27, 2014), and -14.92 m (image pair June 30, 2022 - July 24, 2022). The increasing perpendicular baseline value in the image pair contributes to higher coherence level, indicating the satellite orbit position difference when the image was taken is getting further. Furthermore, the coherence value in the interferogram correlates with the temporal baseline value. Low image coherence can stem from differences in object characteristics from both sides and changes in the observed objects.

Table 3-1. Prependicular Baseline and Temporal Baseline

ID_Scene	Date	Prependicular Baseline	Temporal Baseline
ALPSRP054057100_ALPSRP087607100	January 29, 2007 – September, 16 2007	-670,83 m	230 days
S1A_IW_SLC_20141103T113134_20141127T113133	November 3, 2014 – November 27, 2014	-64,74 m	24 days
S1A_IW_SLC_20220630T113230_20220724T113231	June 30, 2022 – July 24, 2022	-14,92 m	24 days

In the process of InSAR, two satellite images (referred to as the master and slave images) are required in the form of SLC or level 1.0 images. This process results in the generation of an interferogram, which highlights phase and amplitude differences associated with topographic details, deformation effects, noise, and atmospheric disturbances. The technique involves computing changes in distance between the images based on phase information.

The interferogram image is created using InSAR, which involves multiplying corresponding pixels in the master and slave images to obtain phase and amplitude information. The image is then reprocessed to remove topographic effects and obtain a differential interferogram phase and amplitude. This is achieved using a 90 m SRTM DEM for the 2007 interferogram and a 30 m SRTM DEM for the 2014 and 2022 interferograms. An example from 2007 is shown in Figure 3-1.

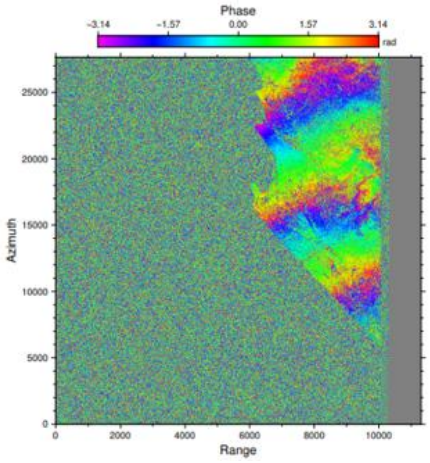

a

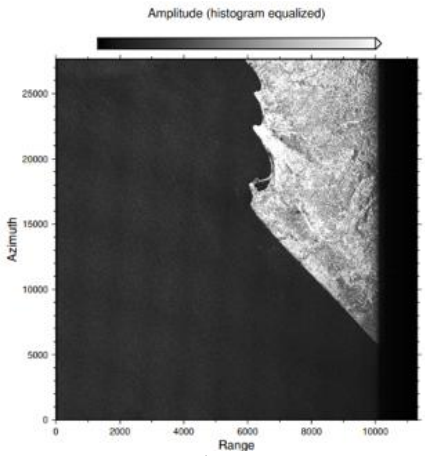

b

Figure 3-1: Interferogram Phase (a) and Amplitude (b) images between January 29 and 16 September 26, 2007

3.2 SAR Image Coherence

The interferometric images generated through the InSAR process exhibit varying degrees of coherence. Coherence represents a quantitative measure used to assess the phase noise present within the interferogram images. Qualitatively, the level of coherence in the imagery can be visually appraised through Figures 3-2 to 3-4.

The interferogram image produced by the InSAR process is generated by cross-multiplying pixels from the master image with those from the slave image. This pixel multiplication yields information that includes both phase and amplitude values. To enhance the accuracy of the results, the interferogram image was reprocessed using the DInSAR technique. This process aims to eliminate the effects of topography, along with applying flattening and filtering. As a

result, the differential interferogram phase and amplitude values are adjusted to remove topographic influences. A 90 m SRTM DEM was used for the 2007 interferogram, while a 30 m SRTM DEM was utilized for the interferograms from 2014 and 2022.

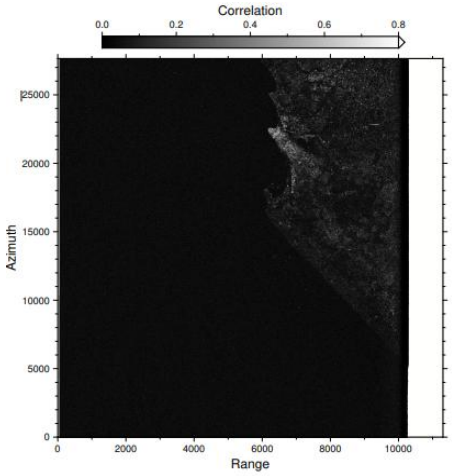

Figure 3-2: Interferogram Image Coherence between January 29 and September 16, 2007

To qualitatively evaluate the coherence of the image, we can analyze the coherence image. In Figures 3-2 to 3-4, the scale bar moving to the right (white) indicates the highest coherence level, whereas the scale bar moving to the left (black) represents the lowest coherence value (Naumowicz et al., 2022). Figures 3-2, 3-3, and 3-4 also show that the coherence image, which appears dark gray tending towards black, has a coherence value below 0.2. Conversely, the light gray region trending towards white indicates a coherence value above 0.2. Areas with coherence values below 0.2 include marine areas and forests with dense vegetation, while coherence values ranging from 0.3 to 0.8 are found in Bengkulu and open areas without forest cover. Low coherence values in interferogram images may be attributed to differences in the characteristics of the two imaging systems involved, such as volumetric scattering or processing errors (Tampuu et al., 2020; Téllez-Quiñones et al., 2020).

Furthermore, the presence of vegetation in the area can also cause low coherence values. Based on the results of SAR data processing, all SAR image pairs exhibit coherence values within the range of 0.00005 to 0.8. This low coherence value results in empty pixels after the image undergoes the unwrapping process.

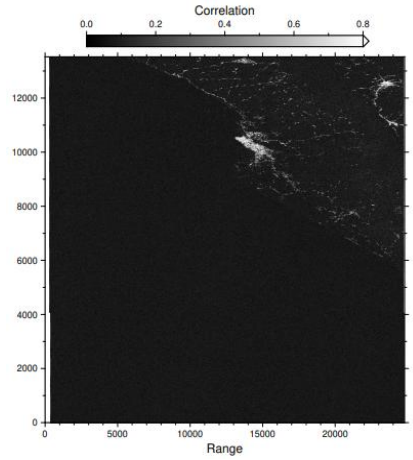

Figure 3-3: Interferogram Image Coherence between November 3 and 27, 2014

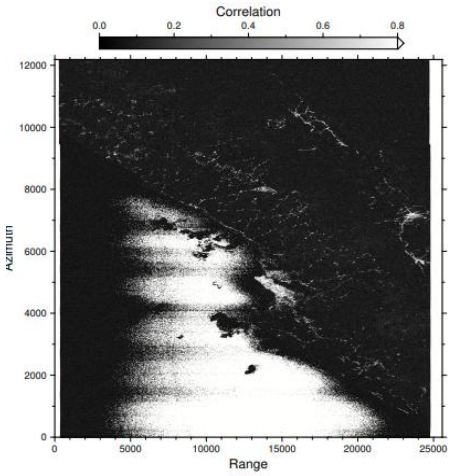

Figure 3-4: Interferogram Image Coherence between June 30 and July 24, 2022

3.3 Unwraping Phase

The interferogram is produced through a flattening process, resulting in an ambiguous measurement due to fringes with a modulo of 2π. To obtain the absolute phase value, an unwrapping process is used to eliminate the ambiguity. Unwrapping is easier in areas with flat surfaces compared to areas with diverse topography (Xu et al., 2023). After the unwrapping process, the interferogram image shows the deformation value in phase (measured in π radians), which is then converted into a deformation value in metric units based on Line of Sight (LOS). The results of this process can be observed in Figure 3-5.

The Bengkulu City area is primarily flat, which influences the results obtained from radar satellite imaging. Flat terrains help minimize distortion in these radar images. Distortion occurs due to two main factors: the incidence angle and the slope of the imaging area. This distortion can significantly impact the unwrapping process, resulting in certain areas appearing blank (a phenomenon known as blank unwrapping).

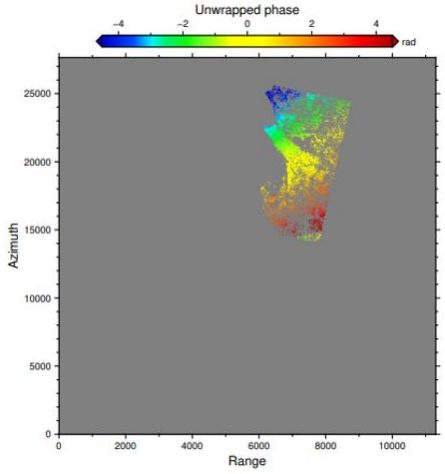

Figure 3-5: Interferogram Image After Unwrapping Process of Image Pair between January 29 and September 16, 2007

3.4 Geocoding

The subsequent step involves generating an interferogram image based on the SAR processing results and subsequently assigning georeferencing according to real-world coordinates. The georeferenced interferogram image is depicted in Figure 3-6. The primary goal of geocoding is to provide geographic context for the DInSAR processing results, allowing for a more accurate analysis and interpretation of deformation data.

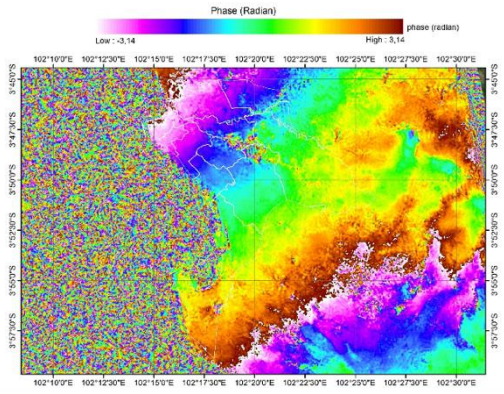

Figure 3-6: Interferogram Phase Image with Coordinate

3.5 Deformation Magnitude Analysis

A cross-section map of the study area was meticulously crafted to precisely determine the magnitude and distribution of deformation values due to earthquakes in the Bengkulu area. The analysis of image pairs processed from January 29, 2007, to September 16, 2007, using the DInSAR method indicated that deformation varied across the cross-sections. Figure 3-7 illustrates two cross-section lines. The North-South cross-section extends from the northern area of Bengkulu City (Muara Bangkahulu District) to the southern area (Kampung Melayu District). In contrast, the West-East cross-section spans from the western part of Bengkulu City (Teluk Segara District) to the eastern part (Selebar District). The findings for the North-South cross-section revealed that the northern region primarily experienced uplift, while the southern region exhibited average subsidence. Conversely, the West-East cross-section demonstrated that the western area experienced average uplift, with only a limited number of areas showing signs of subsidence. As depicted in the graph in Figure 3-8, the North-South cross-section recorded a maximum uplift of 53.4 mm and a minimum of 0.9 mm. For subsidence, the lowest measurement was -0.2 mm, while the highest recorded was -12.8 mm. Meanwhile, the West-East cross-section showed a peak uplift of 56.2 mm and a minimum of 0.3 mm, with subsidence values ranging from -0.5 mm to a maximum of -7.3 mm.

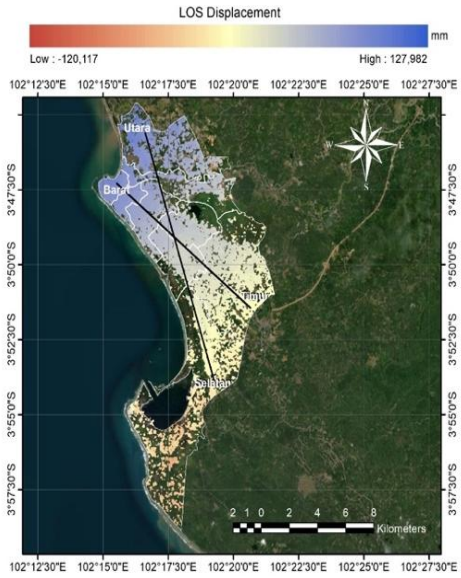

Figure 3-7: Cross-Section Map of Image Pairs between January 29 and September 16, 2007

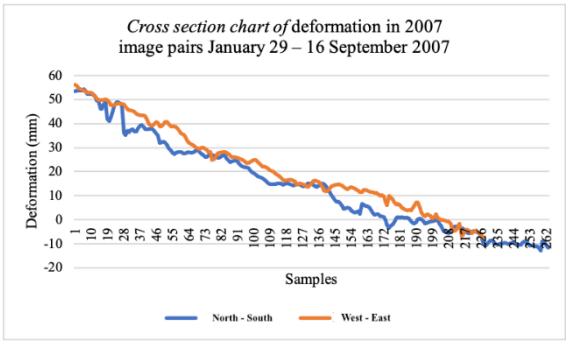

Figure 3-8: Cross-Section Chart of Image Pairs between January 29 and September 16, 2007

The analysis of the image pair processed using the DInSAR method from November 3, 2014, to November 27, 2014, revealed significant variations in deformation along the cross-sections. As illustrated in Figure 3-9, there are two distinct cross-section lines: the North-South cross-section extends from the northern part of Bengkulu City (Muara Bangkahulu District) to the southern part (Kampung Melayu District), while the West-East cross-section runs from the western part (Teluk Segara District) to the eastern part (Selebar District). In the North-South cross-section, the northern region predominantly experienced subsidence, whereas the southern region exhibited an average uplift. In contrast, the West-East cross-section indicated that the western part encountered subsidence, while the eastern part generally displayed uplift.

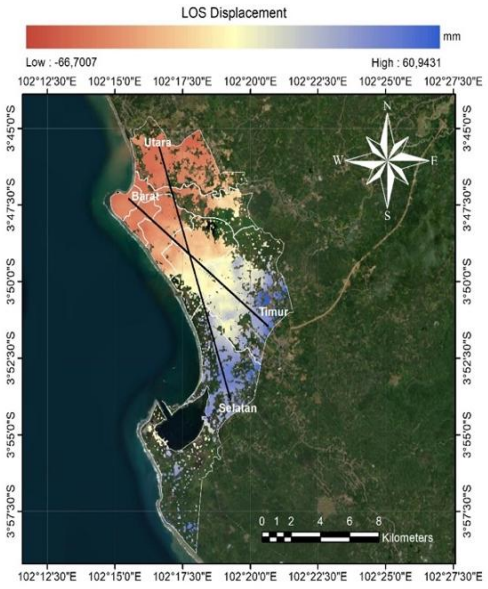

Figure 3-9: Cross-section Map of Image Pairs between November 3 and 27, 2014

According to the data presented in Figure 3-10, the area along the North-South cross-section experienced a maximum uplift of 38.9 mm and a minimum uplift of 0.1 mm. For subsidence, the lowest value recorded was -0.4 mm, with the highest reaching -34.8 mm. In the West-East cross-section area, the maximum uplift observed was 38.4 mm, with a minimum of 0.4 mm, while subsidence ranged from a minimum of -0.3 mm to a maximum of -31.8 mm.

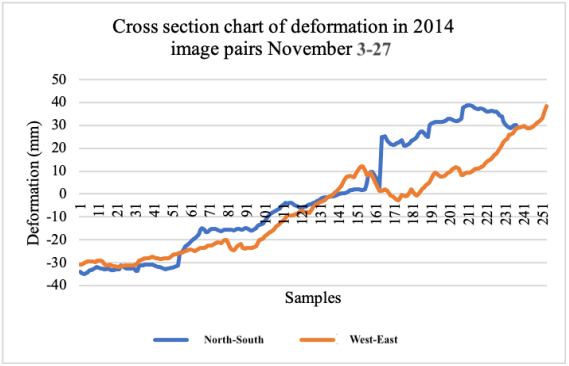

Figure 3-10: Cross-Section Chart of Image Pairs between November 3 and 27, 2014

The analysis of image pairs processed through the DInSAR method from June 30, 2022, to July 24, 2022, revealed significant variation in deformation along the designated cross-sections. Figure 3-11 illustrates two cross-section lines: the North-South cross-section runs from the northern part of Bengkulu City (Muara

Bangkahulu District) to the southern part (Kampung Melayu District), while the West-East cross-section extends from the western part of Bengkulu City (Teluk Segara District) to the eastern part (Selebar District).

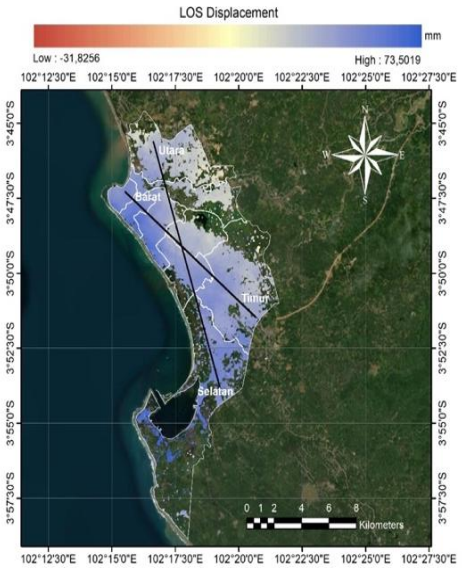

Figure 3-11: Cross-Section Map of Image Pairs between June 30 and July 24, 2022

In both the North-South and West-East cross-sections, all measured areas experienced uplift. As shown in the graph in Figure 3-12, the North-South cross-section recorded uplift throughout all regions, with a minimum value of 32.2 mm and a maximum of 45.2 mm. Likewise, the West-East cross-section demonstrated uplift across all areas, with the lowest value at 31.1 mm and the highest reaching 45.7 mm.

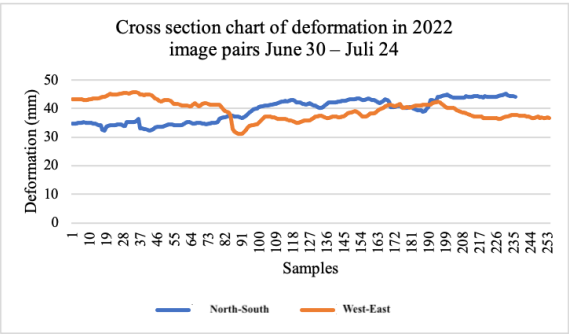

Figure 3-12: Cross-Section Map of Image Pairs between June 30 and July 24, 2022

Based on the findings presented in Table 3-2, it is evident that each earthquake event detected using the DInSAR method results in the accumulation of land surface deformation over a specific time period. Notably, the image pair taken between January 29, and September 16, 2007, exhibits the highest accumulated deformation values, revealing uplifts of 53.4 mm in the Muara Bangkahulu subdistrict and 56.2 mm in the Teluk Segara subdistrict. These values directly correspond to the magnitude of an earthquake on September 12, 2007, which measured 8.6 M_w making it the most powerful earthquake in this study. Similarly, the image pair between June 30 and July 24, 2022, displays the second highest accumulated deformation values, with land surface uplifts of 45.2 mm in the Kampung Melayu subdistrict and 45.7 mm in the Ratu Samban subdistrict, both corresponding to an earthquake on July 20, 2022, with 5.8 M_w. Finally, the image pair captured between November 3 and 27, 2014, shows the smallest accumulated deformation values, with uplifts of 38.9 mm in the Kampung Melayu subdistrict and 38.4 mm in the Selebar subdistrict, related to an earthquake on November 10, 2014, with 4.8 M_w, the smallest earthquake among those in the other time spans.

3.6 Deformed Area Analysis

The earthquake caused significant ground surface deformation in several areas, including most of the Muara Bangkahulu subdistrict, as well as Teluk Segara, Ratu Agung, Ratu Samban, Selebar, and Singaran Pati subdistricts. A small part of the Kampung Melayu subdistrict was also affected. Geological findings indicate that these deformations are strongly linked to fault lines and zones of soil liquefaction.

Understanding these patterns can provide valuable insights for future urban planning. For example, areas with significant deformation should be designated as high-risk zones, which would necessitate stricter building codes to ensure structural resilience. Furthermore, these insights could inform land-use policies to limit development in areas prone to severe ground movement, ultimately helping to mitigate the impact of future seismic events.

3.7 Geological Condition Analysis

According to a survey from the Indonesian Ministry of Energy and Mineral Resources, the geology of the south coast and its surroundings is characterized by Quaternary alluvial and volcanic rocks, as well as Tertiary sedimentary rocks. In Bengkulu, six types of geological formations have been identified: Bintunan formation (QTb), alluvium (Qa), swamp deposit (Qs), alluvium terraces (Qat), swamp sand (Ql), and andesite (Tpan) (see Figure 3-13). The Quaternary and alluvial volcanic rocks are loose, weathered, and poorly composed, and during earthquakes, the sedimentary rocks vibrate strongly but quickly return to their original shape, intensifying the impact of the earthquake shaking.

Tabel 3-2: Comparison of Deformation Values

Image Pairs	*Cross-section* North-South		*Cross-section* West-East	
	***Uplift* (mm)**	***Subsidence* (mm)**	***Uplift* (mm)**	***Subsidence* (mm)**
Image pairs Januar 29 – September 16, 2007	53,4	-12,8	56,2	-7,3
Image pairs November 3 – 27, 2014	38,9	-34,8	38,4	-31,8
Image pairs June 30 – July 24, 2022	45,2	-	45,7	-

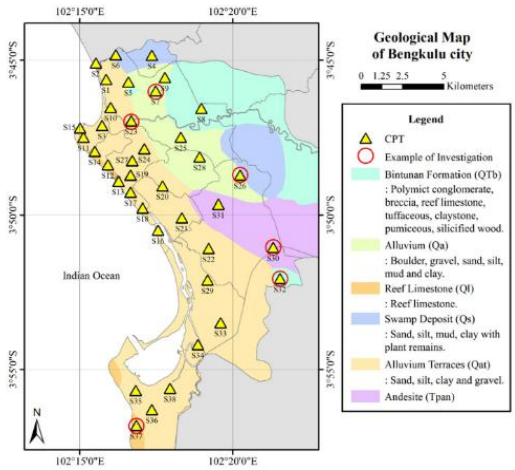

Figure 3-13: Geological Map of Bengkulu City (Mase et al., 2023)

4 CONCLUSION

The research findings indicated that each earthquake event observed using the DInSAR method led to ground surface deformation. The pair of images between January 29 and September 16, 2007 exhibited the highest deformation, with an uplift of 53.4 mm in the Muara Bangkahulu subdistrict and an uplift of 56.2 mm in the Teluk Segara subdistrict. This deformation correlated with the strength of the earthquake that occurred on September 12, 2007, which measured 8.6 M_w, making it the most powerful earthquake in the study. The image pair between June 30 and July 24, 2022 displayed the second highest deformation, with an uplift of 45.2 mm in the Kampung Melayu subdistrict and an uplift of 45.7 mm in the Ratu Samban subdistrict, corresponding to the 5.8 M_w earthquake that occurred on July 20, 2022. The image pair between November 3 and 27, 2014 showed the smallest deformation, with an uplift of 38.9 mm in the Kampung Melayu subdistrict and an uplift of 38.4 mm in the Selebar subdistrict, corresponding to the 4.7 M_w earthquake that occurred on November 10, 2014. The findings underscore the effectiveness of DInSAR in identifying earthquake-related deformations, which can inform local mitigation strategies. Areas exhibiting significant deformation should be prioritized for infrastructure improvements and emergency planning. Future research should focus on the long-term monitoring of deformation trends and the integration of multiple sensors, such as combining DInSAR with optical imagery, to enhance the accuracy and reliability of analyses.

ACKNOWLEDGEMENTS

The research referenced was financially supported by the Department of Research and Community Service at the

University of Bengkulu, under contract number 2950/UN30.15/PT/2024. The authors wish to sincerely acknowledge the provided financial support.

REFERENCES

Anggara, O., Alif, S. M., Lampung, S., History, A., & Deformation, C. (2025). Coseismic deformation of the 2020 bengkulu mw 6.8 earthquake using insar data. *GeoEco*, *11*(1), 62–72.

Asset, A., Khuralay, M., Nabi, N., & Aigerim, K. (2021). Application of GMTSAR and ESA SNAP Software to Determine Earthquake Epicenter Coordinate Using Sentinel-1A/B Radar Remote Sensing Data. *2021 IEEE International Conference on Smart Information Systems and Technologies (SIST)*, 1–6. https://doi.org/10.1109/SIST50301.2021.9465906

Bayik, C. (2021). Deformation analysis of 2020 mw 5.7 Karlıova, Turkey, earthquake using DInSAR method with different incidence angle SAR data. *Arabian Journal of Geosciences*, *14*(4). https://doi.org/10.1007/s12517-021-06670-x

Fielding, E. J., Liu, Z., Stephenson, O. L., Zhong, M., Liang, C., Moore, A., Yun, S. H., & Simons, M. (2020). Surface deformation related to the 2019 Mw7.1 and 6.4 ridgecrest earthquakes in california from GPS, SAR interferometry, and SAR pixel offsets. *Seismological Research Letters*, *91*(4), 2035–2046. https://doi.org/10.1785/0220190302

Goorabi, A. (2020). Detection of landslide induced by large earthquake using InSAR coherence techniques – Northwest Zagros, Iran. *Egyptian Journal of Remote Sensing and Space Science*, *23*(2), 195–205. https://doi.org/10.1016/j.ejrs.2019.04.002

Gusman, A. R., Tanioka, Y., Kobayashi, T., Latief, H., & Pandoe, W. (2010). Slip distribution of the 2007 Bengkulu earthquake inferred from tsunami waveforms and InSAR data. *Journal of Geophysical Research: Solid Earth*, *115*(12), 1–14. https://doi.org/10.1029/2010JB007565

Hakim, W. L., & Lee, C. W. (2020). A review on remote sensing and GIS applications to monitor natural disasters in Indonesia. *Korean Journal of Remote Sensing*, *36*(6–11), 1303–1322. https://doi.org/10.7780/kjrs.2020.36.6.1.3

Kandregula, R. S., Kothyari, G. C., Swamy, K. V., Kumar Taloor, A., Lakhote, A., Chauhan, G., Thakkar, M. G., Pathak, V., & Malik, K. (2022). Estimation of regional surface deformation post the 2001 Bhuj earthquake in the Kachchh region, Western India using RADAR interferometry. *Geocarto International*, *37*(18), 5249–5277. https://doi.org/10.1080/10106049.2021.1899299

Lakhote, A., Thakkar, M. G., Kandregula, R. S., Jani, C., Kothyari, G. C., Chauhan, G., & Bhandari, S. (2021). Estimation of active surface deformation in the eastern Kachchh region, western India: Application of multi-sensor DInSAR technique. *Quaternary International*, *575–576*, 130–140. https://doi.org/10.1016/j.quaint.2020.07.010

Li, Y., Jiang, W., Zhang, J., Li, B., Yan, R., & Wang, X. (2021). Sentinel-1 SAR-Based coseismic deformation monitoring service for rapid geodetic imaging of global earthquakes. *Natural Hazards Research*, *1*(1), 11–19. https://doi.org/10.1016/j.nhres.2020.12.001

Mase, L. Z. (2018). Reliability study of spectral acceleration designs against earthquakes in Bengkulu City, Indonesia. *International Journal of Technology*, *9*(5), 910–924. https://doi.org/10.14716/ijtech.v9i5.621

Mase, L. Z. (2020). Seismic Hazard Vulnerability of Bengkulu City, Indonesia, Based on Deterministic Seismic Hazard Analysis. *Geotechnical and Geological Engineering*, *38*(5), 5433–5455. https://doi.org/10.1007/s10706-020-01375-6

Mase, L. Z. (2023). Identification of potential seismic damage in Tanah Patah area, Bengkulu City, Indonesia. *Acta Geodaetica et Geophysica*, *58*(3), 389–412.

https://doi.org/10.1007/s40328-023-00419-6

Mase, L. Z. (2024). A Case Study of Liquefaction Potential Verification During a Strong Earthquake at Lempuing Subdistrict, Bengkulu City, Indonesia. *Transportation Infrastructure Geotechnology*, *11*(4), 1547–1572. https://doi.org/10.1007/s40515-023-00335-w

Mase, L. Z., Agustina, S., Hardiansyah, Farid, M., Supriani, F., Tanapalungkorn, W., & Likitlersuang, S. (2023). Application of Simplified Energy Concept for Liquefaction Prediction in Bengkulu City, Indonesia. *Geotechnical and Geological Engineering*, *41*(3), 1999–2021. https://doi.org/10.1007/s10706-023-02388-7

Mase, L. Z., Wahyuni, M. S., Hardiansyah, & Syahbana, A. J. (2024). Prediction of Damage Intensity Level Distribution in Bengkulu City, During the Mw 8.6 Bengkulu-Mentawai Earthquake in 2007, Indonesia. *Transportation Infrastructure Geotechnology*, *11*(2), 769–793. https://doi.org/10.1007/s40515-023-00306-1

Murjaya, J., Rahman, A. S., Sili, P. D., Karnawati, D., Supriyanto, Fatimah, S., Sutiyono, Sugianto, D., & Ahadi, S. (2023). Earthquake Risk Potential Caused by Active Faults in Sumatra (Case Study: Earthquakes in the Land of West Sumatra Province and its vicinity). *IOP Conference Series: Earth and Environmental Science*, *1244*(1). https://doi.org/10.1088/1755-1315/1244/1/012037

Naumowicz, B., Wieczorek, B., & Pelc-Mieczkowska, R. (2022). Possibility of using the DInSAR method in the development of vertical crustal movements with Sentinel-1 data. *Open Geosciences*, *14*(1), 1290–1309. https://doi.org/10.1515/geo-2022-0401

Nurtyawan, R., & Yulanda, M. F. (2020). Lombok earthquakes using DInSAR techniques based on Sentinel 1A data (case study: Lombok, West Nusa Tenggara). *IOP Conference Series: Earth and Environmental Science*, *500*(1). https://doi.org/10.1088/1755-1315/500/1/012065

Razi, P., Sumantyo, J. T. S., Izumi, Y., Tadono, T., Mizukami, Y., Ohki, M., & Motohka, T. (2023). Estimation of Potential Earthquake Epicenter Based on Level of Land Deformation Along Coastal Line of South Java. *International Geoscience and Remote Sensing Symposium (IGARSS)*, *2023–July*, 8194–8197. https://doi.org/10.1109/IGARSS52108.2023.10282176

Sattler, K., Elwood, D., Hendry, M. T., Berscheid, B., Marcotte, B., Abdulrazagh, P. H., & Huntley, D. (2022). Field Collection of Geotechnical Measurements for Remote or Low-Cost Datalogging Requirements. *Geotechnical Testing Journal*, *45*(1), 59–78. https://doi.org/10.1520/GTJ20200323

Suhadha, A. G., & Julzarika, A. (2022). Dynamic Displacement using DInSAR of Sentinel-1 in Sunda Strait. *Trends in Sciences*, *19*(13), 1–11. https://doi.org/10.48048/tis.2022.4623

Tampuu, T., Praks, J., Uiboupin, R., & Kull, A. (2020). Long term interferometric temporal coherence and DInSAR phase in Northern Peatlands. *Remote Sensing*, *12*(10), 7–9. https://doi.org/10.3390/rs12101566

Téllez-Quiñones, A., Salazar-Garibay, A., Valdiviezo-Navarro, J. C., Hernandez-Lopez, F. J., & Silván-Cárdenas, J. L. (2020). DInSAR method applied to dual-pair interferograms with Sentinel-1 data: a study case on inconsistent unwrapping outputs. *International Journal of Remote Sensing*, *41*(12), 4662–4681. https://doi.org/10.1080/01431161.2020.1727056

Usman, F., Syamsir, A., & Melasari, J. (2022). *Mapping of Earthquake-Induced Land Deformation on Urban Area Using Interferometric Synthetic Aperture Radar Data of Sentinel-1 BT - Recent Advances in Earthquake Engineering* (S. Kolathayar & S. C. Chian (eds.); pp. 491–502). Springer Singapore.

Vatresia, A., Utama, F. P., Hati, I. P., & Mase, L. Z. (2024). Discovering Bengkulu Province Earthquake Clusters with CLARANS Methods. *Journal of Soft Computing in Civil Engineering*, *8*(3), 71–86. https://doi.org/10.22115/scce.2023

.381204.1589

Xu, Y., Lu, Z., Bürgmann, R., Hensley, S., Fielding, E., & Kim, J. (2023). P-band SAR for ground deformation surveying: Advantages and challenges. *Remote Sensing of Environment*, *287*(June 2022), 113474. https://doi.org/10.1016/j.rse.2023.113474

Yang, R., Huang, J., & Griffiths, D. V. (2022). Optimal geotechnical site investigations for slope reliability assessment considering measurement errors. *Engineering Geology*, *297*(December 2020), 106497. https://doi.org/10.1016/j.enggeo.2021.106497